

EFFECTS OF CLIMATE CHANGES ON WATER AVAILABILITY IN CENTRAL EUROPE

J. MIKA^{1,2}, ILONA PAJTÓK-TARI¹, G. VARGA¹, G. BÁLINT³



ABSTRACT. – Effects of projected climate changes both on average conditions and extremes are investigated by the use of global climate models of the IPCC AR4 (2007). Computed changes in 21 coupled ocean-atmosphere general circulation models (OAGCM) are first analysed for periods 2080-2099 and 1980-1999, focusing on hydrology related parameters, including precipitation, runoff, mean temperature, diurnal temperature range, cloud coverage and soil moisture. In a wide sub-set of the models, the decrease of runoff indicates lower amount of water energy. A few percent of decrease is projected in the soil moisture, as well. The precipitation and temperature results, including their inter-model variance and change of temporal variability projected by the same global models additionally are adjusted to the 2030-2049 time slices, selected for flood hazard assessment. The MAGICC/SCENGEN 5.3v2 diagnostic model (Wigley, 2008) is used to adjust the model results to the external forcing alternatives and time-horizons. The projections are based on the moderately rapid A1B emission scenario, and a mitigation-oriented scenario postulating climate stabilisation at the 450 ppm equivalent CO₂-scenario. Spatial resolution of both OAGCM-based scenarios is 2.5 x 2.5 deg. which is enough to describe robust features of the water balance. The inter-model variability of the sea-level pressure changes indicates that even the embedded mezo-scale models, not used in the present study, are not fully sound tools for regional climate projections. The study is closing by the discussion of the strong inter-model differences in the pressure changes, providing the boundary conditions for the next, mezo-scale generation of the regional climate models.

1. INTRODUCTION

Water resources of the Carpathian Basin are dominated by transit flow coming from the neighbouring mountainous regions. The region is very sensitive to floods of the streams arriving to the territory. This corresponds also to long-term changes considered to be related to global climate changes. Hydrological scenarios, therefore, can not be complete without estimation of regional climate changes in the distant up-stream regions of the Upper Danube watershed.

IPCC Third Assessment Report suggests that similarly to many regions of the World, eastern and central European countries could become vulnerable to the global warming. Many investigations support these findings e.g. in the Carpathian Basin: next to rising temperature means, severe shortage of precipitation occurred in the last few decades, therefore, ecosystems is facing to high risk of ecological

¹ Department of Geography, Eszterházy Károly College, Eger, Hungary

² Hungarian Meteorological Service, Budapest, Hungary

³ VITUKI Environmental Protection and Water Management Research Institute, Budapest, Hungary



changes, as well. Parallel to the changes of precipitation, that are not unequivocal in space (e.g. Mika and Balint, 2000), frequent extreme events (e.g., floods with fast runoff and persistent droughts) may occur, result in unstable climate conditions and increased vulnerability of water management in the region. These facts highlight the importance of detailed climate research of the region.

In the allotted space one can find the brief specification of the 21 global climate models with their Institution, vertical and horizontal resolutions. Average changes based on all available output fields are presented for to indicate future changes in water availability.

2. RESULTS FROM THE GENERAL CIRCULATION MODEL OUTPUTS (2080-2099)

In the recent IPCC Report (2007) Chapter 10 displays maps of changes of several climate variables. The model simulations are based on the mid-range (A1B) SRES scenario (Nakicenovic and Swart, 2000). The forecasted and control periods are 2071-2100 vs. 1980-1999. The main features of the models are listed in Table 1. Majority of the models are new compared to the previous IPCC Report. In some cases, similar models of the same institute are used with differences in the resolution, or in parameterization of one single process.

Table 1. The mapped OAGCMs (IPCC 2007 WG-I, Ch. 8, 597-599 (www.ipcc.ch)).
The order of information: host-institution, upper boundary (top), vertical and horizontal resolution in atmosphere (A) and ocean (O).

AVERAGE RESPONSE = average of the max. 21 available model responses	GISS-AOM, 2004: NASA Goddard Institute for Space Studies, USA, top = 10 hPa, L12 A: 3° x 4° O: 3° x 4° L16
GISS-EH, 2004: NASA Goddard Institute for Space Studies, USA, top = 0.1 hPa, L20 A: 4° x 5° O: 2° x 2° L16	GISS-ER, 2004: NASA Goddard Institute for Space Studies, USA, top = 0.1 hPa L20 A: 4° x 5° O: 4° x 5° L13
GFDL-CM2.0, 2005: NOAA/Geophysical Fluid Dyn. Lab., USA top = 3 hPa L24, A: 2.0° x 2.5° O: 0.3°-1.0° x 1.0°	GFDL-CM2.1, 2005 NOAA/Geophysical Fluid Dyn. Lab., USA, =GFDL-CM2.0 with semi-Lagrangian atmospheric transport
CGCM3.1(T47), 2005: Canad. Centre for Clim. Mod. Anal., Canada, top =1 hPa, L31 A: T47 (~2.8° x 2.8°) O: 1.9° x 1.9° L29	CGCM3.1(T63), 2005: Canad. Centre for Clim. Mod. Anal., Canada, top =1 hPa, L31 A: T63 (~1.9° x 1.9°), O: 0.9° x 1.4° L29
MIROC3.2(hires), 2004: U.Tokyo; Nat. Ins. Env. Stud.; JAMSTEC, Japan top =40 km, L56 A: T106 (~1.1° x 1.1°) O: 0.2° x 0.3° L47	MIROC3.2(medres), 2004: U.Tokyo; Nat. Ins. Env. Stud.; JAMSTEC, Japan top = 30 km L20 A: T42 (~2.8°x2.8°) O: 0.5°-1.4°x1.4° L43
UKMO-HadCM3, 1997: Hadley Centre / Meteorol. Office, UK top =5 hPa, L19 A: 2.5° x 3.75° O: 1.25° x 1.25° L20	UKMO-HadGEM1, 2004: Hadley Centre/ Meteorol. Office, UK top = 39.2 km, L38 A: ~1.3° x 1.9° O: 0.3°-1.0° x 1.0° L40
CCSM3, 2005: National Center for Atmosph. Res., USA, top = 2.2 hPa, L26 A: T85 (1.4°x1.4°), O: 0.3°-1°x1°, L40	CNRM-CM3, 2004: Météo-France/Centre Nat. Rech. Mét.. France, top =0.05 hPa L45, A: T63 (~1.9° x 1.9°) O: 0.5°-2° x 2° L31

CSIRO-MK3.0, 2001: <i>Comm. Sci. Industr. Res. Org., Australia</i> , top = 4.5 hPa, L18 A: T63 (~1.9° x 1.9°) O: 0.8° x 1.9° L31	ECHAM5/MPI-OM, 2005: <i>Max Planck Inst. f. Meteor., Germany</i> , top =10 hPa, L31 A: T63 (~1.9° x 1.9°), O: 1.5° x 1.5° L40
ECHO-G, 1999 <i>Meteor. Inst. Univ. Bonn, FRG, Met. Res. Inst. Korea</i> , top =10 hPa L19 A: T30 (~3.9°x3.9°) O: 0.5°-2.8°x2.8° L20	FGOALS-g1.0, 2004: <i>Nat. Key Lab. /Inst. Atmos. Phys., China</i> , top = 2.2 hPa, L26 A: T42 (~2.8° x 2.8°) O: 1.0° x 1.0° L16
INM-CM3.0, 2004: <i>Institute for Numerical Mathematics, Russia</i> top = 10 hPa, L21 A: 4° x 5° O: 2° x 2.5° L33	IPSL-CM4, 2005: <i>Institut Pierre Simon Laplace, France</i> top = 4 hPa, L19 A: 2.5° x 3.75° O: 2° x 2° L31
MRI-CGCM2, 2003: <i>Meteorological Res. Institute, Japan</i> top = 0.4 hPa L30 A: T42 (~2.8°x2.8°) O: 0.5°-2.0°x2.5° L23	PCM, 1998: <i>National Center for Atmosph. Research, USA</i> top = 2.2 hPa L26 A: T42 (~2.8°x2.8°) O: 0.5°-0.7°x1.1° L40

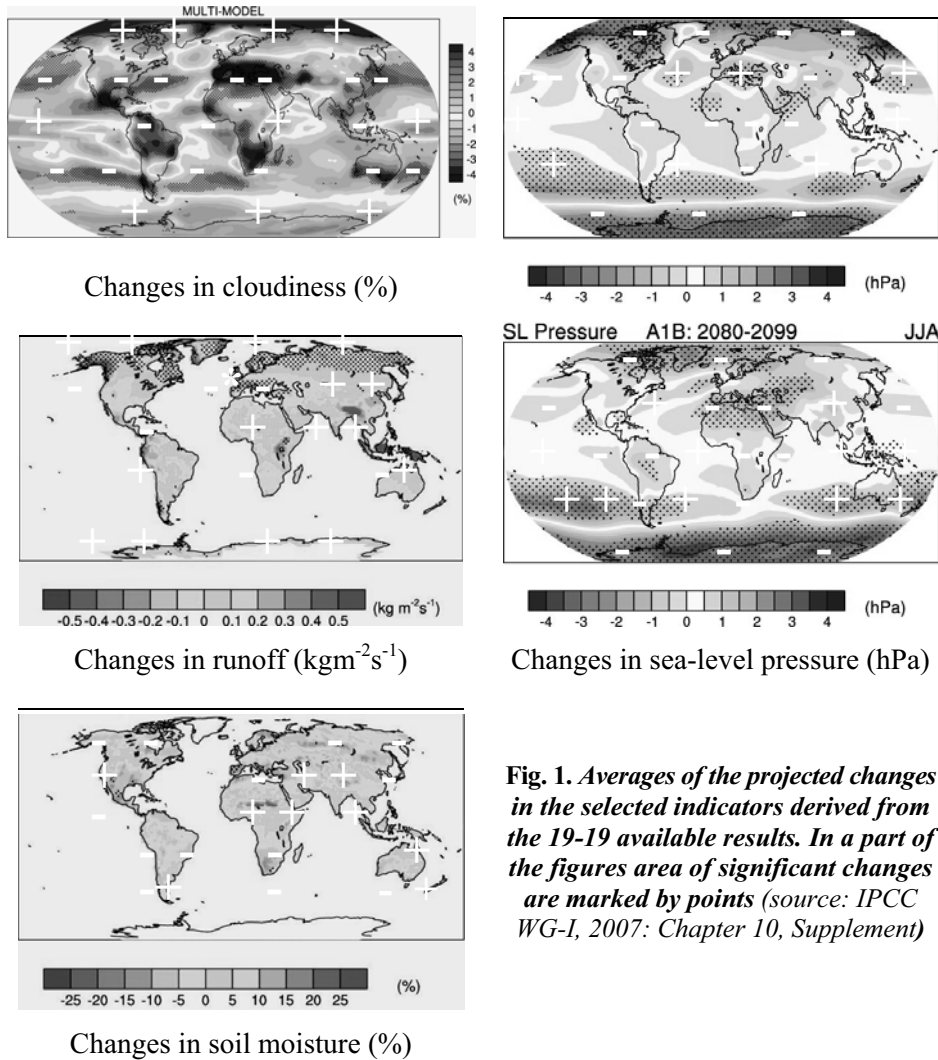


Fig. 1. Averages of the projected changes in the selected indicators derived from the 19-19 available results. In a part of the figures area of significant changes are marked by points (source: IPCC WG-I, 2007: Chapter 10, Supplement)



In Figure 1 the average changes in cloudiness, sea-level pressure, runoff and soil-moisture content are presented. Except the pressure changes, all values are annual averages. In various 2-2 models there were no results published in the given source. According to the remained 19-19 model outputs, slightly more solar energy is expected in East-Central Europe. Decrease of the wind speed would occur in the winter period with a partial compensation in summer. The increase of the sea-level pressure in winter implies weaker wind from the large-scale circulation and less intense convective activity, but in summer the tendencies are the opposite. In a wide sub-set of the models, the decrease of runoff indicates lower amount of water energy. A few percent of decrease is projected also in the soil moisture. The large characteristic sizes of the changes with identical signs are due to coarse resolution of the models and the averaging.

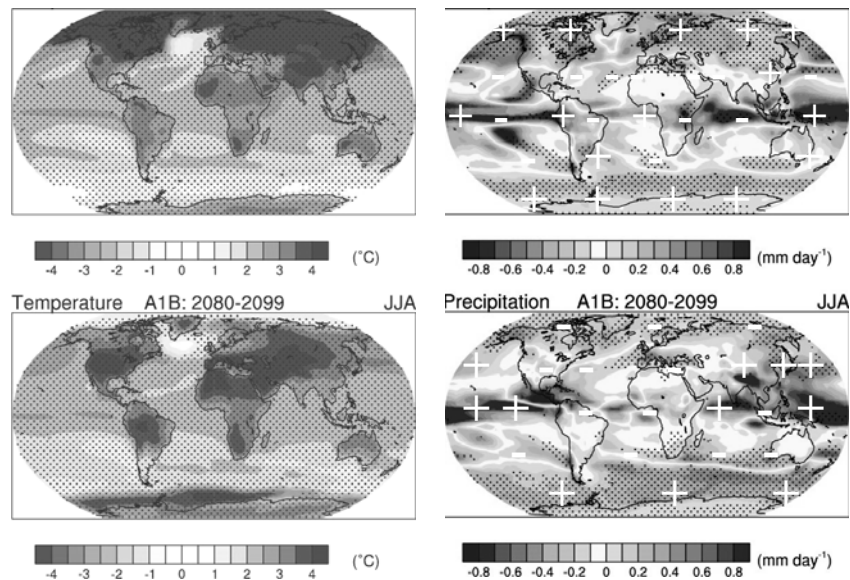


Fig. 2. Model average changes of temperature (warming everywhere) and precipitation (see the signs). Both maps are easy to interpret in physical geography

3. INTER-MODEL VARIABILITY OF THE PRESSURE CHANGES

In the previous Section we presented the average changes, but the individual model responses may exhibit fairly large differences. Hence, (i) no single GCM output can be applied to make adaptation-related consequences (in our respect on availability of water resources), and (ii) the embedded regional climate models aimed to overcome the differences between the GCM-resolution and the significant scales, are strongly influenced by the boundary conditions. This is demonstrated in Fig. 3, where the air pressure changes are presented in two almost identical models. The differences are considerable even in the sign of the patterns. This means, that though joining of GCMs with regional models (Christensen et al.,



2007; Halenka and Jacob, 2008) promise better results, we should not forget the uncertainty of the mainframe GCMs.

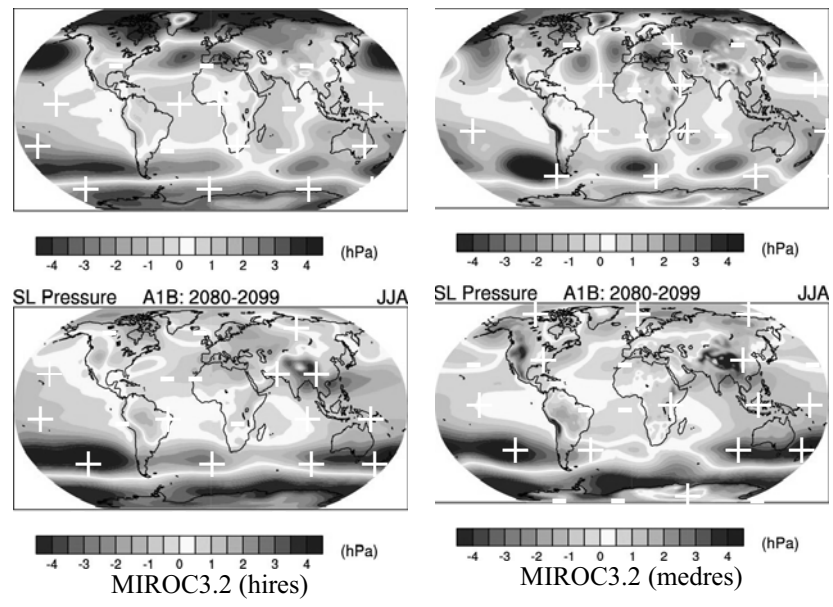


Fig. 3. Comparison of pressure changes fields in a pair of almost identical models, differing only in horizontal and vertical resolution. The upper graphs are winter, the lower ones are summer. The results diverge in the East-Central European sector

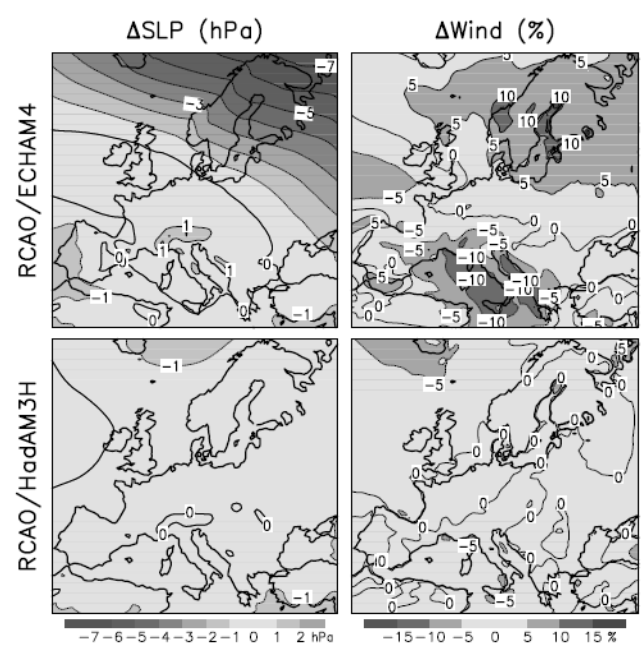


Fig. 4. Simulated changes in annual mean sea-level pressure (Δ SLP) and the near-surface wind speed (Δ Wind) for 2071-2100 compared to 1961-1990, according to the A2 emission scenario. The results are obtained by regional atmosphere-ocean model of the Rossby Centre, Stockholm in both cases. In the upper cases the boundary conditions were provided by the ECHAM4/OPYC3 mainframe model. In the lower cases, this role was performed by the HadAM3H model. The corresponding changes considerably differ from each other. (Fig. 11.6 of the IPCC, 2007)

This role is clearly demonstrated in Fig. 4, where two different mainframe models (Hadley Centre of the British MetOffice and Max Planck Institute for Meteorology) led to different response in the same regional model (Rossby Centre, Stockholm). The projected changes in the wind speed are much more expressed, though of different sign, in the upper combination of the models than in the lower one.

4. DIAGNOSTIC RESULTS FROM THE *MAGICC/SCENGEN V.5.3*

In order to generate climate scenario on local and regional scales, a relatively simple tool, namely, the *MAGICC/SCENGEN 5.3* software package (Wigley et al., 2003, 2008) was applied. All these newest GCMs were evaluated by the Fourth Assessment Report (IPCC, 2007). The global section of the package, the *MAGICC*, is based on an upwelling diffusion energy balance model calibrated by global sensitivity of the GCMs outputs (Fig. 5). For a selected region, the large number of GCM output fields may reduce the existing uncertainty of climate prediction.

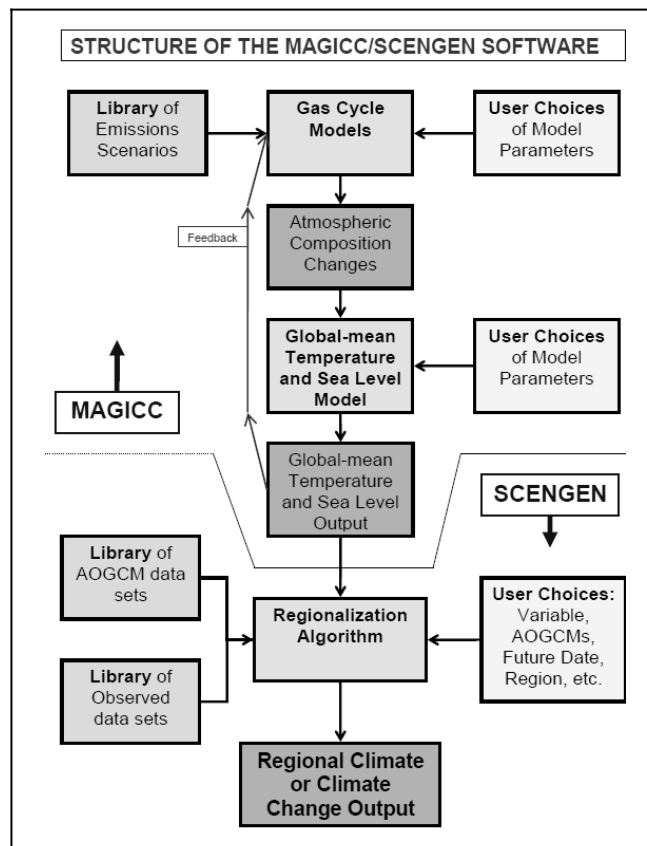
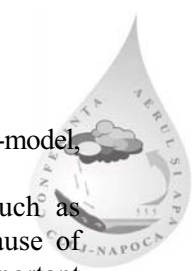


Fig. 5. A schematic diagram showing the main inputs, operations and outputs of *MAGICC/SCENGEN 5.3* (Wigley, 2008)



In this section 20 GCMs treated by the package are considered. (The oldest GISS-model, the GISS-ER, 2004 was omitted from the models of Table 1.)

Local climate change is strongly influenced by local features such as mountains, which are not well represented in global climate models because of their coarse resolution. Yet, despite these deficiencies, GCMs play an important role in regional climate research. In the followings the same model outputs, with one exclusion, are obtained and synchronised by the MAGICC/SCENGEN 5.3 diagnostic software tool. One must note that the SCENGEN software applies linear scaling from one given set of output fields from each model.

Figures 6 and 7 demonstrate the seasonal changes in temperature and in precipitation for the European sector, respectively. The maps are rather patchy, intentionally not smoothed, though the MAGICC/SCENGEN software provides this alternative, in order to document the real resolution of the whole GCM-based approach. (Here the detailed analysis of the fields does not really allow to supply the BW maps even with the signs. Moreover, in case of temperature the warming is almost identical.) One should note that these maps are derived from the above GCM-outputs but linearly scaled to a more practical time period, closer (still from above) to the scope of the long-term water management and planning.

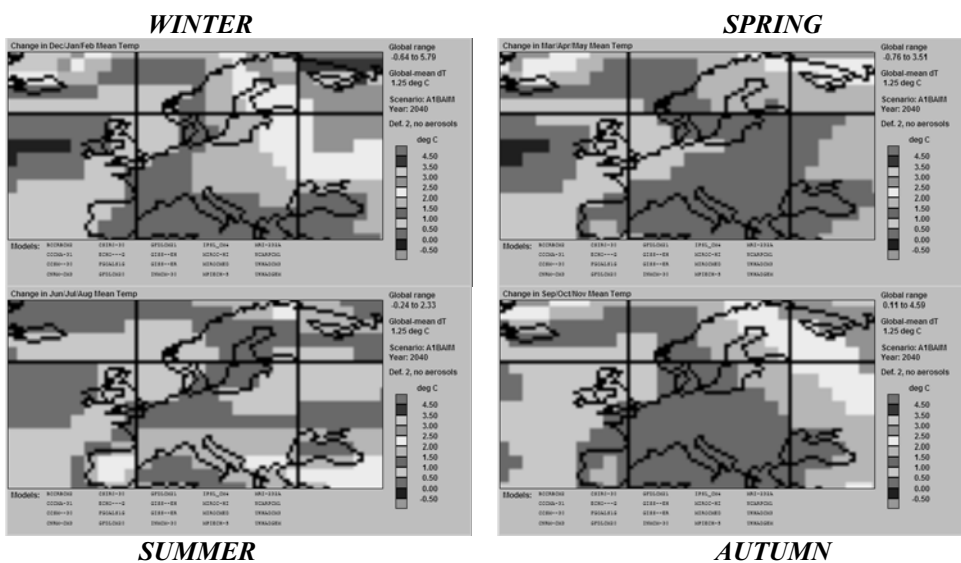


Fig. 6. Model-mean changes of temperature computed by the MAGICC/SCENGEN for 2030-2049 compared to 1980-1999. The projected global change is 1.25 K. The strongest warming areas are found in the north-east and north-west sectors of the European region. The less warming is seen in the Atlantic with almost no change.

Besides the precipitation as the key of the water income and the temperature, regulating the evapotranspiration, the latter term is also influenced by the direct energy balance depending on cloudiness. However, cloudiness is far not the strongest side of the GCMs, due, again, to comparably coarse resolution.

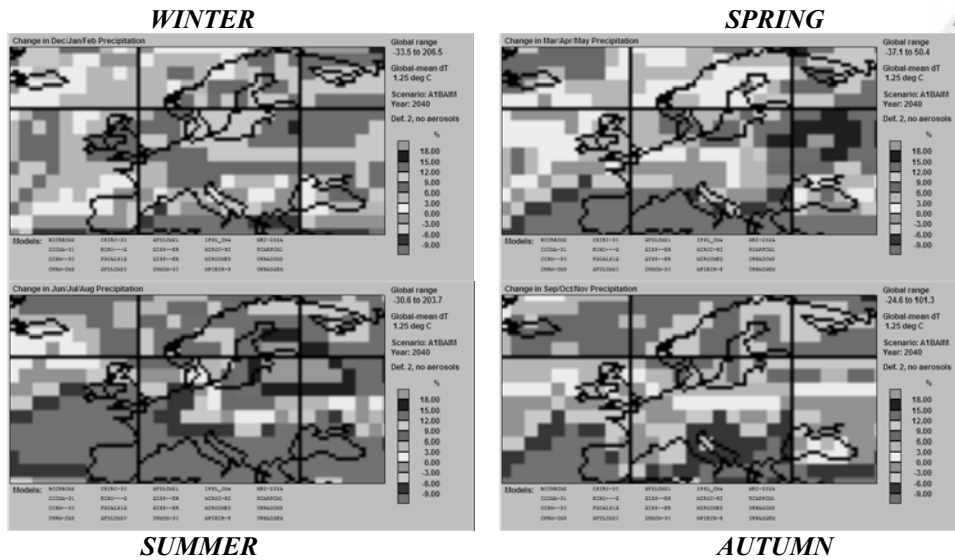


Fig. 7. Model-mean changes of precipitation computed by the MAGICC/SCENGEN for 2030-2049 compared to 1980-1999. The projected global change is 1.25 K. The southern areas become drier, but the northern, especially north-eastern sectors get wetter. The exact borders between these sectors are varying with the seasons. In summer and in autumn the Alpine-Carpathian region should expect a decrease in precipitation but it is partly compensated in the rest of the year.

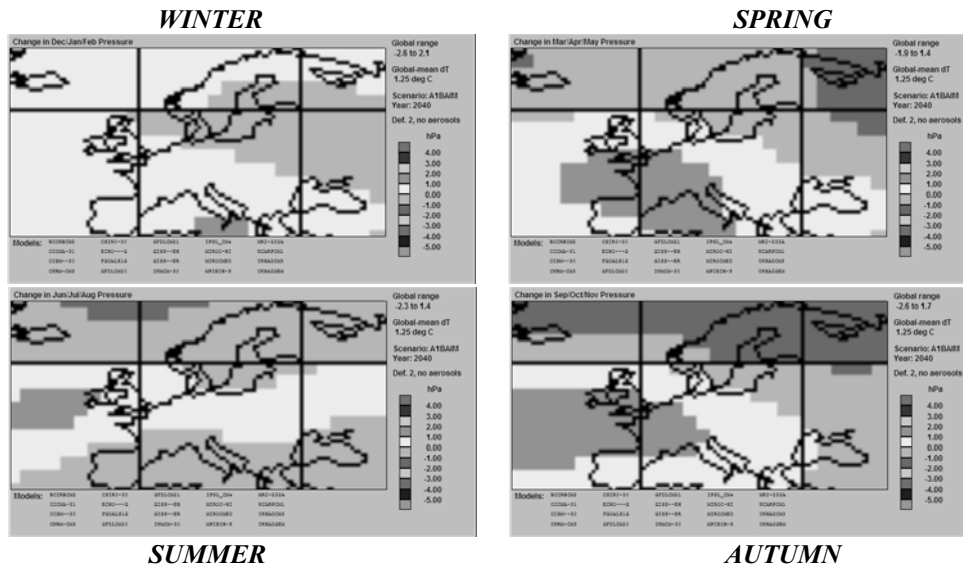


Fig. 8. The MAGICC/SCENGEN 5.3 model-mean changes of the sea-level pressure for 2030-2049 compared to 1980-1999. The projected global change is 1.25 K. The air pressure above the Alpine-Carpathian region increases in all seasons, especially in spring and autumn, in connection with the intensifying Azores-maximum.



Therefore most of the modelling groups avoid publishing the cloudiness changes in their models. This is the case with the MAGICC/SCENGEN (integrating the individual GCM-versions), hence we should limit ourselves at studying the changes in the sea-level pressure (Fig. 8). If doing it, we must establish that in all seasons the sea-level pressure would increase in the Alpine Carpathian region. Hence, this component may shift the water balance towards further decreasing of the water balance.

In conclusion, the average water balance is going to shrink, though about the frequency of individual high-water cases one should rely on models with finer resolution, despite the difficulties of this kind of modelling, partly demonstrated in Section 3.

REFERENCES

1. Christensen, J.H., Carter T.R., Rummukainen, M. and Amanatidis, G. 2007. *Predicting of regional scenarios and uncertainties for defining European climate change risks and effects: The PRUDENCE Project*. Climatic Change 81: Suppl., 1-371.
2. Halenka, T. and Jacob, D., (eds.), 2008: *Workshop on Regional Climate Modeling. Időjárás*, vol. 112, No. 3–4,
3. IPCC, 2007: *Climate Change 2007: The Physical Science Basis*. Contribution of WG-I to the Fourth Assessment Report of the IPCC, Cambridge University Press, 996 pp.
4. Mika J. and Bálint G., 2000: *Rainfall scenarios for the Upper-Danube catchment. XXth Conf. Danubian Countries*, Bratislava, Slovakia, 4-8 September, 2000. CD-ROM, pp. 990-995
5. Nakicenovic, N. and Swart, R. (eds.), 2000: *Emissions Scenarios: A Special Report of Working Group III of the Intergovernmental Panel on Climate Change*. Special Report on Emissions Scenarios. Cambridge Univ. Press, Cambridge - New York, 612 pp.
6. Wigley, T.M.L., 2003: *The MAGICC/SCENGEN Climate Scenario Generator: Version 4:1 User Manual*.
7. Wigley, T.M.L., 2008: *MAGICC/SCENGEN 5.3: User Manual (version 2)* 1-81 pp.